HARNESSING CONVEX OPTIMIZATION TECHNIQUES FOR IMAGE DENOISING

Guruprasanna Rajukannan Suresh (21051075)
Mukund Sayeganesh Chettiar (21051147)
Sindhuja Chaduvula (21051129)

1 INTRODUCTION

In the realm of Digital Image Processing, the presence of noise in visual data often poses significant challenges. Noisy artifacts, introduced through various means, can greatly affect an image's interpretability and visual appeal. At the core of addressing this problem lies the process of 'Image Denoising'. This process is implemented to remove or at least minimize such unwanted noise, all while ensuring that the intrinsic structures and details inherent to the image remain unaffected.

There are several types of noise, but two of the most common noises are Gaussian and Salt-and-Pepper noise. Gaussian noise is characterized by its randomness in altering pixel values, governed by a Gaussian distribution. This kind of noise tends to spread across the image often giving it a blurred or foggy appearance. Salt-and-Pepper noise, contrasting sharply with Gaussian noise, isn't diffused across the image. Instead, it occasionally introduces glaring black-and-white pixels. It can be visualized as if someone has sprinkled salt and pepper across the image, leading to stark, isolated disturbances.

Given the challenges posed by these noise types, researchers have delved deep into developing robust denoising techniques. Among these, techniques based on convex optimization have gained prominence due to their effectiveness and mathematical elegance. Already existing methods of prominence in this domain include the total variation approach and the quadratic filter method. As part of our study, we use these noises for evaluation of the proposed algorithm [1].

1.1 QUADRATIC FILTERING (QF)

In the domain of signal processing, Quadratic Filtering stands out as a straightforward technique. This method is designed to minimize the Euclidean norm of a signal's gradient while attempting to make minimal alterations to the actual signal [2]. Mathematically, this can be captured as:

$$\min_{\hat{x}} \|\hat{x} - x_{\text{corr}}\|_2^2 + \lambda \sum_{i=0}^{n-1} (\hat{x}_{i+1} - \hat{x}_i)^2 \tag{1}$$

In this equation, x_{corr} represents the original signal with noise, $\hat{x}$ denotes the denoised signal, n is the signal's length, and λ serves as a hyperparameter determining the balance between signal smoothing and conserving its inherent structure.

The term $\sum_{i=0}^{n-1} (\hat{x}_{i+1} - \hat{x}_i)^2$ is essentially the squared Euclidean norm of the gradient, represented as

$$\|\nabla x_{\text{corr}}\|_2 = \left(\sum_{i=0}^{n-1} (\hat{x}_{i+1} - \hat{x}_i)^2 \right)^{1/2}. \tag{2}$$

This formulation is a bi-criterion convex optimization task since both of its components are convex by nature [2]. Given the inherent simplicity and wide application in one-dimensional denoising, it's tempting to extend this approach to two-dimensional image processing. Doing so, the problem can be formulated as:

$$\min_{\hat{I}} \|\hat{I} - I_{\text{corr}}\|_{\text{sq}} + \lambda \|\nabla_x \hat{I}\|_{\text{sq}} + \lambda \|\nabla_y \hat{I}\|_{\text{sq}} \tag{3}$$

where $\hat{I}$ is the denoised or processed image, I_{corr} is the original noisy image, and λ is the regularized hyperparameter. Here, $\|A\|_{\text{sq}} = \sum_{i,j} A_{ij}^2$ specifies the sum-of-squares norm for a matrix. The symbols ∇_x and ∇_y indicate the gradients concerning the x and y dimensions, respectively. An empirical observation is that this two-dimensional adaptation tends to induce a significant blurring effect on images, a drawback that's also evident in its one-dimensional counterpart [2].

1.2 TOTAL VARIATION FILTERING (TVF)

Some denoising techniques, such as the quadratic filter, tend to over-simplify images, leading to unwanted blurriness. By tweaking the underlying optimization principles, this shortcoming can be addressed. An effective substitute for the quadratic penalization approach involves using the image's total variation, often seen in one-dimensional data as the accumulated absolute gap between neighbouring points [1].

$$\text{TV}(x) = \sum_i |x_{i+1} - x_i| \tag{4}$$

Here, x is a one-dimensional sequence, and x_i is the value of the sequence at the i-th position. Expanding this concept to two-dimensional images, the TVF algorithm can be articulated as:

$$\min_{\hat{I}} \left\| \hat{I} - I_{\text{corr}} \right\|_{\text{sq}} + \lambda \left\| \hat{I} \right\|_{\text{TV}} \tag{5}$$

where $\hat{I}$ is the processed image, I_{corr} is the original noisy image, λ is the hyperparameter. The TV norm, $\|A\|_{\text{TV}}$, can be defined using the gradient differences:

$$\|A\|_{\text{TV}} = \left(\sum_{i,j} \left((A_{i+1,j} - A_{i,j})^2 + (A_{i,j+1} - A_{i,j})^2 \right) \right)^{1/2} \tag{6}$$

Where A represents an image. Nevertheless [3], this quadratic form is computationally intensive. A more ubiquitous version employs absolute differences:

$$\|A\|_{\text{TV}} = \sum_{i,j} |A_{i+1,j} - A_{i,j}| + |A_{i,j+1} - A_{i,j}| \tag{7}$$

This version reduces image blur significantly but might introduce artifacts, often described as a 'staircase' effect. Even though this method of total variation offers computational benefits, optimizing it remains non-trivial. Here's where advanced optimization techniques like the primal-dual algorithm come into play. Specifically designed for problems of the form [4]:

$$\min_x F(Kx) + G(x) \tag{8}$$

In this context, F and G represent convex functions, with K acting as a linear operator. By applying specific transformations and leveraging the convex conjugate of F, we can reframe the issue into a min-max format, enhancing its solvability. A pivotal component in this methodology is the proximal operator, which facilitates the iterative resolution of numerous convex dilemmas. Using methods like the Arrow-Hurwicz version of the primal-dual, as opposed to direct solvers like cvxpy [5], the optimization becomes considerably faster without compromising the accuracy of the results. Such advancements underscore the significance of leveraging the inherent structure of convex problems for effective and efficient solutions.

1.3 EXACT MATRIX COMPLETION (EMC)

Exact Matrix completion methods capitalize on the natural low-rank attributes of images and shine particularly when a significant number of data points are absent, making them a top pick for operations like image inpainting [6]. In this study, we devise a denoising technique based on Exact Matrix Completion and perform analysis with the existing methods.

2 LITERATURE REVIEW

Image denoising is a fundamental problem in the field of image processing that seeks to enhance the quality of images by reducing unwanted noise while preserving important details. The roots of this problem trace back to the early days of photography and image capture when technological limitations often resulted in noisy and degraded images. However, the recognition of this issue and the development of solutions gained significant momentum with the advancement of digital imaging technologies.

In medical imaging, clarity and accuracy are paramount for sound diagnosis. Noisy medical images, if left untreated, could lead to misdiagnosis and compromised patient care. Denoising techniques, such as total-variation denoising [1], have emerged as vital tools in ensuring that crucial medical information remains unobscured, safeguarding patient well-being. The domain of security surveillance is similarly impacted. Surveillance systems grappling with noisy images face obstacles in accurately identifying potential threats. Effective denoising [4] enhances image quality, thereby aiding in the identification and apprehension of potential risks. Additionally, the significance of image denoising extends to the realm of art restoration. Historical artifacts and artworks, corroded by the passage of time and noise, lose their intrinsic allure. Denoising techniques, influenced by seminal research such as Candès and Tao's work on matrix completion (2010) [7], emerge as restorative tools, enabling conservators to peel back the layers of time and reveal the original splendour of artworks.

2.1 EXPLORATION OF TECHNIQUES, OPTIMIZATION METHODS, AND STANDARDS IN IMAGE DENOISING

A multitude of image-denoising techniques have been developed to address the persistent challenge of noise reduction. These solutions span diverse approaches, each with its strengths and limitations. Total variation denoising [1] minimizes total variation to preserve edges and structures. However, its performance falters in textured regions. Non-local means denoising [8] averages similar patches to optimize image details while reducing noise. Wavelet denoising [9] attenuates noise in specific frequency bands using wavelet transforms.

These techniques involve finding optimal solutions that minimize objective functions while adhering to constraints. Total variation denoising itself is rooted in convex optimization. This paper [4] introduces an algorithmic framework that optimizes dual functional and primal images concurrently. This exemplifies the prowess of optimization in solving image restoration challenges. Matrix completion techniques [7] deploy optimization principles to recover low-rank matrices from sparse observations. While not solely intended for denoising, the optimization-centric approach resonates with the problem by capitalizing on inherent image structure. Furthermore, "Matrix Completion with Noise" [10] offers a nuanced perspective on matrix completion under noise, enhancing our understanding of optimization-based denoising strategies.

For the purpose of comparative analysis, we have chosen three reference methods to gauge the effectiveness of our proposed innovations in image denoising. First, the total variation filtering, rooted in convex optimization principles, excels in preserving edges while reducing noise, although it may struggle with textured regions [1]. Second, the quadratic filter technique offers a variational approach to noise reduction [11]. Still, its limitations can arise when addressing complex noise patterns and intricate structures. Third, our innovation involves leveraging exact matrix completion which is originally intended for finding missing elements in a matrix, and harnesses the low-rank structure of images to address denoising [6]. This approach holds the potential to preserve both global and local image structures. These reference methods collectively serve as benchmarks to assess our proposed advancements, facilitating a comprehensive evaluation of their respective capabilities and limitations in diverse image-denoising scenarios.

3 PROPOSED SOLUTION

In this section, we introduce a strategy for addressing image denoising through the lens of exact matrix completion [6]. Our approach revolves around treating the pixels within a degraded-quality image as the missing elements in a matrix. To restore these pixels, we harness the power of Exact Matrix Completion, transforming the problem into a convex optimization paradigm. This formulation allows us to efficiently estimate the missing pixel values and thereby enhance the overall quality of the image.

We assume that images can be approximated as matrices with low-rank characteristics. In other words, the underlying image matrix $\boldsymbol{X}$ possesses a relatively small rank. We also make the presumption that the input image M contains only a few observations Ω which preserve the image quality. Our objective is to reclaim a low-rank matrix structure from a subset of entries that are considered to retain the image quality. This is formulated as a rank minimization problem given as

$$\begin{aligned} &\text{Minimize } \operatorname{rank}(\boldsymbol{X}) \\ &\text{Subject to } \boldsymbol{X}_{ij} = \boldsymbol{M}_{ij},\ (i,j) \in \Omega \end{aligned} \tag{9}$$

where $\boldsymbol{X} \in \mathbb{R}^{m \times n}$, and $\mathcal{R}_\Omega$ denotes a sampling operator in the observed region Ω.

As the rank minimization problem is NP-hard because of the discontinuous and non-convex nature of the rank, the nuclear norm (sum of singular values of the matrix $\boldsymbol{X}$) is used as it is the convex envelope of the matrix rank [12]. This leads us to the nuclear norm minimization formulation:

$$\begin{aligned} &\text{Minimize } \|\boldsymbol{X}\|_* \\ &\text{Subject to } \boldsymbol{X}_{ij} = \boldsymbol{M}_{ij},\ (i,j) \in \Omega \end{aligned} \tag{10}$$

In our pursuit of optimization, we decompose $\boldsymbol{X}$ using Singular Value Decomposition (SVD):

$$\boldsymbol{X} = \boldsymbol{U}\Sigma\boldsymbol{V}^* \tag{11}$$

We define $\boldsymbol{W}_1 = \boldsymbol{U}\Sigma\boldsymbol{U}^*$ and $\boldsymbol{W}_2 = \boldsymbol{V}\Sigma\boldsymbol{V}^*$ as the constituent matrices. This facilitates our introduction of $\boldsymbol{Y}$, preserving the essence of $\boldsymbol{X}$ while simplifying optimization by ensuring its nuclear norm equates to the nuclear norms of constituent matrices $\boldsymbol{W}_1$ and $\boldsymbol{W}_2$:

$$\boldsymbol{Y} = \begin{bmatrix} \boldsymbol{W}_1 & \boldsymbol{X} \\ \boldsymbol{X}^* & \boldsymbol{W}_2 \end{bmatrix} \tag{12}$$

with the following properties satisfied:

$$\|\boldsymbol{X}\|_* = \|\boldsymbol{W}_1\|_* = \|\boldsymbol{W}_2\|_* \tag{13}$$

Additionally, the trace of $\boldsymbol{Y}$ can be expressed as the sum of the traces of $\boldsymbol{W}_1$ and $\boldsymbol{W}_2$, which equates to twice the nuclear norm of $\boldsymbol{X}$:

$$\operatorname{trace}(\boldsymbol{Y}) = \operatorname{trace}(\boldsymbol{W}_1) + \operatorname{trace}(\boldsymbol{W}_2) = 2\,\|\boldsymbol{X}\|_* \tag{14}$$

Thus, the reduced form of nuclear norm minimization is obtained and we introduce an additional constraint for our use case of image denoising by formulating the minimization problem as the following:

$$\begin{aligned} \text{Minimize} \quad & \|\boldsymbol{Y}\|_* \\ & \boldsymbol{Y}_{ij} = \boldsymbol{M}_{ij},\ (i,j) \in \Omega \\ \text{Subject to} \quad & \boldsymbol{Y} = \boldsymbol{Y}^T \\ & \boldsymbol{Y} \succeq 0 \end{aligned} \tag{15}$$

The first equality constraint ensures that for each observed pixel entry provided in the set that is considered to preserve the image quality, equality is imposed to ensure that the corresponding entry in $\boldsymbol{Y}$ matches the observed value from the original image $\boldsymbol{M}$. The second symmetric equality constraint is considered here to ensure that the reconstructed matrix remains symmetric throughout the optimization process. This constraint aligns with the underlying assumption that real-world matrices, including images, exhibit symmetry. In the context of image denoising or matrix completion, this constraint helps maintain the structural coherence of the image during the reconstruction process. Assuming that the matrix is positive semidefinite ensures compatibility with convex optimization methods. Positive semidefiniteness guarantees that the matrix's eigenvalues are non-negative, aligning with the convex nature of optimization. This assumption simplifies the optimization landscape. Additionally, it enforces stability and meaningful solutions in the reconstruction process, aiding in preserving image structure while filling in missing or degraded regions. Thus, the matrix $\boldsymbol{Y}$ is constrained to be both symmetric and positive semidefinite (PSD), which makes this a Semi-Definite Program.

After the completion of the optimization process, the reconstructed image is obtained by extracting the top right corner of the solved matrix $\boldsymbol{Y}$ as the matrix shown in Eq 12. For our analysis, we consider the images to be symmetric and reshape them before applying the algorithm in order to maintain the symmetric property. This approach is consistent with the formulation of the convex optimization problem and ensures that the output of the algorithm is the reconstructed image, with the degraded parts filled in based on the optimization process.

The proposed exact matrix completion algorithm offers a robust and efficient solution to the problem of image denoising by reconstructing the image. By leveraging convex optimization techniques, we recover the image while adhering to observed entries and exploiting the inherent low-rank structure. The algorithm's performance is demonstrated through experiments on various images for salt and pepper noise and Gaussian noise. The results are compared with the Quadratic Filtering and Total Variation Filtering methods on the basis of the Peak Signal-To-Noise Ratio.

4 EXPERIMENTAL RESULTS

In our study, we focus on two prevalent noise types affecting images: Salt-and-Pepper noise and Gaussian noise. The salt-and-pepper noise, an impulse or spike noise, is marked by random appearances of white (salt) and black (pepper) pixels. This noise type transforms select pixels entirely to black or white. This disruption is commonly attributed to malfunctioning camera sensors or transmission hiccups, manifesting as conspicuous white and black dots on images, demanding distinct corrective strategies due to its pronounced effects. On the other hand, Gaussian noise is an additive disturbance influenced by a bell-curve distribution. It typically results from electronic disruptions in devices like digital cameras or scanners, leading to slight, pervasive changes across every pixel, rendering images with a grainy texture and reduced sharpness.

Expanding on our earlier discussion about Gaussian and Salt-and-Pepper noise, our study explored ways to combat these issues. In our research, we looked into three denoising methods: Quadratic Filter(QF) and Total Variation Filtering (TVF), which are well known, and our proposed method, Exact Matrix Comple-

Salt-and-Pepper Noise												
Images	p = 0.05				p = 0.1				p = 0.2			
	Noise	QF	TVF	EMC	Noise	QF	TVF	EMC	Noise	QF	TVF	EMC
Bridge	18.55	22.42	21.67	40.84	15.64	22.78	21.48	38.08	12.82	22.89	10.99	34.24
Couple	18.77	20.88	24.46	43.29	15.89	20.58	23.36	39.81	13.09	19.14	21.35	36.38
Clock	18.07	22.19	22.1	42.7	15.04	22.76	21.72	39.16	12.28	22.4	19.52	35.41
Peppers	18.1	23.23	24.22	41.32	15.38	22.13	22.31	40.42	12.53	20.95	19.51	33.9

Table 1: Comparison of PSNR scores for denoising methods for different p (noise ratio) values.

Gaussian Noise												
Images	σ = 0.01				σ = 0.025				σ = 0.05			
	Noise	QF	TVF	EMC	Noise	QF	TVF	EMC	Noise	QF	TVF	EMC
Bridge	14.65	19.24	18.99	18.04	13.09	15.3	14.92	16.77	11.92	13.02	12.82	16.11
Couple	18.03	16.74	18.22	20.43	15.44	15.03	18.01	19.68	13.13	13.5	17.36	18.96
Clock	15.89	17.56	16.77	18.3	14.14	13.93	13.04	17	12	11.34	10.82	15.61
Peppers	15.58	15.92	15.62	17.36	10.98	12.4	11.6	14.38	12.79	13.82	13.28	15.19

Table 2: Comparison of PSNR scores for denoising methods for different σ (variance) values.

tion (EMC). With its inherent simplicity, QF delicately enhances the image, holding the authenticity of the original signal paramount. Conversely, the TV places emphasis on safeguarding distinct image contours, effectively mitigating sudden pixel disruptions. The EMC method taps into the foundational low-rank characteristics of pristine images, striving for a flawless noise-free reconstruction. During practical tests on four distinct grayscale images, we evaluated these methods under varying noise ratios for salt-and-pepper noise and varying variance for Gaussian noise, measuring the outcomes of the techniques with the Peak Signal-to-Noise Ratio (PSNR), the results obtained for the Pepper image has been shown in Figure 1. PSNR quantifies the denoised image's quality by contrasting the potential maximum signal strength against the influence of the interfering noise. Superior image quality after denoising is indicated by a greater PSNR value.

4.1 SALT AND PEPPER NOISE

In our study, we tested images with three levels of salt-and-pepper noise ratio: 0.05, 0.1, and 0.2. Our results displayed in Table 1 show clear differences in how various denoising methods performed for salt-and-pepper noise. Notably, the EMC method consistently showcased superior performance across all noise levels. When subjected to p = 0.05, the EMC algorithm yielded remarkable PSNR scores of 40.84, 43.29, 42.7, and 41.32 for the Bridge, Couple, Clock, and Peppers images, respectively. Similarly, at p = 0.1 and p = 0.2, the EMC algorithm exhibited considerable noise reduction prowess, outshining QF and TVF methods.

On the other hand, the TVF and QF methods performed comparatively lower than the EMC algorithm. Examining the overarching patterns, it becomes evident that the EMC method outperformed others across all levels of noise, underscoring its robustness in handling disruptive noise. This observation is clearly illustrated in Figure 2 depicting average results under the influence of salt and pepper noise. In contrast, the TVF and QF methods exhibited relatively diminished performance compared to the EMC algorithm. This is because salt and pepper noise harshly impacts certain pixels but leaves others untouched. EMC operates on the principle that despite some pixels being corrupted, the true structure of the data can be reconstructed using the remaining data. Thus, EMC does better reconstruction in this case by considering the pixels affected by salt and pepper noise as the missing pixels and then reconstructing the image. The TVF and QF methods underperform primarily due to their less adaptive handling of localized, disruptive noise like

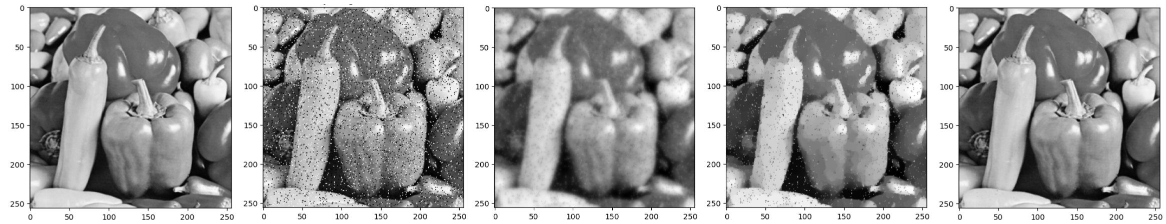

(a) Original (b) Noise (18.1) (c) QF (23.23) (d) TVF (24.22) (e) EMC (41.32)

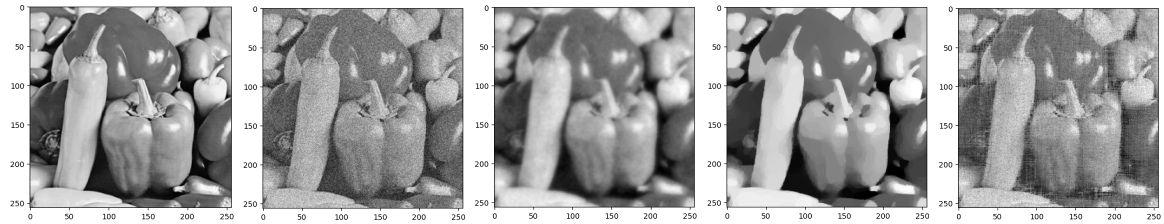

(f) Original (g) Noise (15.58) (h) QF (15.92) (i) TVF (15.62) (j) EMC (17.36)

Figure 1: Comparison of PSNR scores for different denoising techniques such as QF, TVF, and EMC for Salt and Pepper Noise (top row) and Gaussian Noise (bottom row)

salt-and-pepper, which requires a more holistic data reconstruction approach.

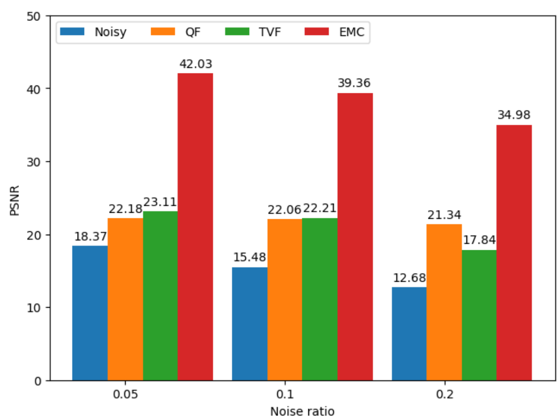

(a) Salt and pepper noise

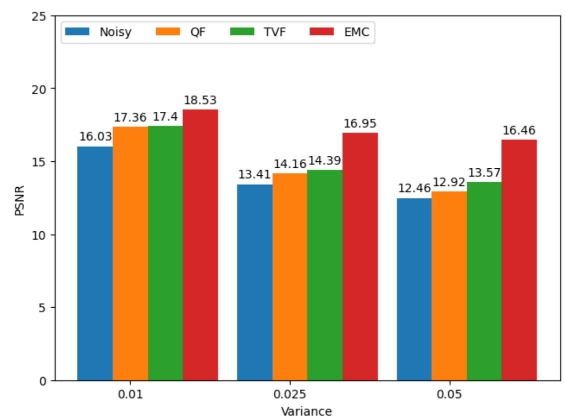

(b) Gaussian noise

Figure 2: Comparison of Average PSNR for denoising techniques for Salt and pepper noise and Gaussian noise

4.2 GAUSSIAN NOISE

In our study involving Gaussian noise, the denoising techniques displayed varying performance levels as displayed in Table 2. Notably, at $\sigma = 0.01$, the EMC method exhibited PSNR scores of 18.04, 20.43, 18.3, and 17.36 for the Bridge, Couple, Clock, and Peppers images, respectively. As the variance increased to $\sigma = 0.025$ and $\sigma = 0.05$, the EMC algorithm consistently demonstrated competitive noise reduction capabilities, though experiencing a decrease in PSNR scores. All 3 methods provide more or less similar performance with EMC being the dominant among them.

In summary, TVF showcased its strength predominantly at milder noise levels, especially with specific images that can be seen in Figure 2. In contrast, as the noise got more intense, EMC's PSNR score in handling it became increasingly clear, leading the pack at the highest noise level tested. However, the performance of EMC may still need to be improved for Gaussian Noise. On the other hand, the QF technique seemed to perform a bit less impressive than EMC and TVF. Gaussian noise behaves differently with each image and denoising technique due to its inherent characteristics and the way each method deals with this type of noise. Since it is characterized by its random distribution, it introduces variations based on Gaussian distribution so each and every pixel might be affected. Gaussian noise alters all these attributes differently, making certain images harder or easier to restore based on their details.

5 DISCUSSION AND CONCLUSION

In the process of image denoising, especially when subjected to varying noise intensities and types, the importance of employing a robust technique is necessary. Our experiments have brought forth some interesting findings. Most notably, EMC has been distinguished as a top-notch way to denoise noisy images, exhibiting a consistent performance across different images and noise conditions. Its ability to adapt and effectively denoise, regardless of its intensity makes it a reliable technique for image denoising, although there is some potential improvement that can be done for Gaussian Noise. We also looked at two other denoising techniques QF and TVF methods, even though they are effective in their own ways, their performance varied in more complex situations. Their effectiveness seemed to change depending on the specific image we were working on and the kind of noise it had. This suggests that while QF and TV can be a good denoising technique in certain situations, they might not always be the best fit for every noisy image problem we encounter.

As we look towards future research, we are interested in the performance evaluation of EMC by using more advanced algorithms like the Alternating Direct Method of Multipliers(ADMM) [13] and the Proximal Gradient method [14]. ADMM is a powerful optimization algorithm that decomposes complex problems into easier-to-solve sub-problems through iterative processes whereas, the proximal gradient method is an optimization technique ideal for problems with non-smooth constraints, leveraging the 'proximity' operator to converge to a solution iteratively. By using these cutting-edge algorithms, we might be able to make EMC perform even better or find ways to improve the other methods.

REFERENCES

[1] L. Rudin, S. Osher, and E. Fatemi, "Nonlinear total variation based noise removal algorithms," *Physica D: Nonlinear Phenomena*, vol. 60, pp. 259–268, 11 1992.

[2] S. Boyd and L. Vandenberghe, *Convex Optimization*. Cambridge University Press, 2004.

[3] L. Condat, "Discrete total variation: New definition and minimization," *SIAM Journal on Imaging Sciences*, vol. 10, no. 3, pp. 1258–1290, August 2017.

[4] A. Chambolle and T. Pock, "A primal-dual algorithm for total-variation-based image restoration," *SIAM Journal on Imaging Sciences*, vol. 3, no. 4, pp. 856–877, 2011.

[5] S. Diamond and S. Boyd, "Cvxpy: A python-embedded modeling language for convex optimization," 2016.

[6] E. J. Candes and B. Recht, "Exact matrix completion via convex optimization," 2008.

[7] E. J. Candès and T. Tao, "Matrix completion from a few entries," *IEEE Transactions on Information Theory*, vol. 56, no. 6, pp. 2980–2998, 2010.

[8] A. Buades, B. Coll, and J.-M. Morel, "A non-local algorithm for image denoising," in *2005 IEEE Computer Society Conference on Computer Vision and Pattern Recognition (CVPR'05)*, vol. 2, 2005, pp. 60–65 vol. 2.

[9] D. L. Donoho and I. M. Johnstone, "Adapting to unknown smoothness via wavelet shrinkage," *Journal of the American Statistical Association*, vol. 90, no. 432, pp. 1200–1224, 1995.

[10] R. Keshavan, A. Montanari, and S. Oh, "Matrix completion from a few entries," *Information Theory, IEEE Transactions on*, vol. 56, pp. 2980 – 2998, 07 2010.

[11] T. F. Chan and J. Shen, *Image Processing and Analysis: Variational, PDE, Wavelet, and Stochastic Methods*. Society for Industrial and Applied Mathematics, 2005.

[12] B. Recht, M. Fazel, and P. A. Parrilo, "Guaranteed minimum-rank solutions of linear matrix equations via nuclear norm minimization," *SIAM Review*, vol. 52, no. 3, pp. 471–501, 2010.

[13] R. Taleghani and M. Salahi, "An admm-factorization algorithm for low rank matrix completion," vol. 14, pp. 1145–1156, 12 2019.

[14] Q. Wang, W. Cao, and Z. Jin, "Two-step proximal gradient algorithm for low-rank matrix completion," *Statistics, Optimization Information Computing*, vol. 4, 06 2016.